

Ultra-Fast DNA Separations Using Capillary Electrophoresis

Karel Klepárník, Odilo M. Mueller, and František Foret

1. Introduction

For decades electrophoresis, together with chromatography and centrifugation, has been one of the most important tools in biochemistry and biology. Size selective separations using synthetic polyacrylamide sieving gels (SDS-PAGE) (1), development of the two dimensional electrophoresis (2D-PAGE) (2) together with the use of the polyacrylamide gels for DNA sequencing (3,4) revolutionized the field of bio-separations (5–7). At present, slab-gel electrophoresis is the most frequently used technique for analysis of proteins and DNA. At the same time, it is also laborious and relatively slow since only low electric field strength can be applied without excessive Joule heating. Numerous efforts to increase the separation speed have been taken, typically applying very thin gel slabs, allowing higher electric field strength during the separation.

Alternative approach for fast electrophoresis utilized a narrow capillary as the separation column. This technique was pioneered by Hjertén (8) and Virtanen (9) and refined by Mikkers (10) and Jorgenson (11). Although capillary electrophoresis (CE) first emerged as a free solution technique, sieving media for size selective separations have been developed soon after (12). It is worth mentioning that the first papers on electrophoresis in gel-filled capillaries had been published in the early 1960s when the term “capillary gel electrophoresis” had also been used for the first time (13–14). Although the potential of capillary gel electrophoresis has clearly been demonstrated in these early works and even instrumentation for multiple CE was developed, the lack of a suitable detector prevented any practical success and the works have been forgotten for the next two decades.

At present, CE is a mature technique routinely applied for inorganic, organic, environmental, pharmaceutical, and biological analyses. The potential for very high separation speed and multiplexing, together with sensitive laser-induced fluorescence (LIF) detection make the technique ideal for a number of applications in DNA analysis. The

From: *Methods in Molecular Biology*, Vol. 163:
Capillary Electrophoresis of Nucleic Acids, Vol. 2: *Practical Applications of Capillary Electrophoresis*
Edited by: K. R. Mitchelson and J. Cheng © Humana Press Inc., Totowa, NJ

development of replaceable sieving matrices (**12**) allows reusing the separation column for hundreds of consecutive runs. This enables the use of completely automated systems that were previously impossible with the slab gels. The separation of DNA fragments by capillary array electrophoresis (CAE) is currently having an increasing impact on the speedy completion of the Human Genome Project.

Most CE separations are performed using columns of 25–50 cm long with typical analysis time on the order of tens of minutes. However, in many cases, the analysis time can be substantially shortened simply by decreasing the separation distance, increasing the electric field strength, or both. The reduction of the separation time, resulting in increased analysis throughput, is of great importance. Much shorter analysis times can be achieved easily with miniaturized instrumentation, using either standard capillary columns, or micro fabricated chips. This chapter aims at reviewing the principles and limitations of CE for ultra-fast DNA separations using replaceable sieving matrices.

1.2. Practical Considerations for Fast DNA Separations

A series of experimental factors have to be considered for fast DNA separations, where the goal is to achieve resolution of two consecutive zones in a minimum amount of time. From the definition of migration time t (Eq. 1), it is evident that effective capillary length and electrical field strength are two key parameters which influence the speed of a separation.

$$t = \frac{l_{\text{eff}}}{\mu \cdot E} \quad (1)$$

The symbols in equation 1 are: l_{eff} = effective capillary length, E = electric field strength, and μ = electrophoretic mobility of the analyte.

Decreasing the separation distance (effective capillary length) and increasing the applied electrical field strength will result in a decrease in the separation time. Clearly, there are fundamental limitations as to how fast a DNA separation can be. First, the production of Joule heat is the restrictive factor that limits the electric field strength. For any given applied electrical field strength, the smaller the dimensions of the separation system, the lower the electric current generated. This dictates the application to systems with a minimal cross-sectional area of the separation channel.

Another factor limiting the speed of analysis is the zone dispersion during the separation. For practical description, it is useful to relate the zone width (in the form of a variance of the zone concentration distribution σ^2) to the length of the separation column l^2 as the separation efficiency, N . The separation efficiency scales with the capillary length as:

$$N = \frac{l_{\text{eff}}^2}{\sigma_{\text{tot}}^2} = \frac{l_{\text{eff}}^2}{\sigma_{\text{ext}}^2 + \sigma_{\text{diff}}^2 + \sigma_{\text{therm}}^2 + \sigma_{\text{other}}^2} \quad (2)$$

where σ_{tot}^2 is the total peak variance, σ_{ext}^2 is the extra column dispersion, σ_{diff}^2 is the diffusion dispersion, σ_{therm}^2 is the thermal dispersion, and σ_{other}^2 is dispersion caused by other factors. Clearly, if short separation distances are to be used, each source of dispersion has to be minimized to achieve high separation efficiencies.

To characterize the practical consequence of zone dispersion, one can follow electrophoretic separation of two DNA species with the zone resolution, R_s , defined in terms of selectivity, α , and separation efficiency, N :

$$R_s = \frac{1}{4} \cdot \frac{\Delta\mu}{\mu} \cdot \sqrt{N} = \frac{1}{4} \cdot \alpha \cdot \sqrt{N} \quad (3)$$

in which $\Delta\mu = \mu_2 - \mu_1$ is the difference in the electrophoretic mobilities of the separated DNA species, and μ is the average mobility of the two species. In **Eq. 2**, the selectivity term is independent from the capillary length. However, because of the dynamic nature of DNA molecules (changes in DNA conformation), the selectivity is a function of the applied electric field strength (**15**). In general, selectivity can decrease significantly by increasing the applied electric field strength to more than few hundred V/cm.

1.2.1. Extra-Column Dispersion

The extra-column effects due to the original size of the injected sample, σ_{inj}^2 , and the finite size of the detection spot, σ_{det}^2 , are independent of the electric field strength and the separation time. In miniaturized systems, where the contribution of time dependent dispersions is minimized by the short analysis time, the extra-column dispersion effects can be dominant (**16**). The contribution of LIF to the extra-column dispersion can also be minimized by use of a detection spot size of 10–50 μm . On the other hand, sample injection varies greatly and can have a significant impact on the resolution. It is, therefore, important to inject only a very narrow injection plug, if high-speed DNA separations are to be achieved with sufficient resolution. Since the DNA sample is typically introduced by electromigration, a narrow injection plug can be generated by use of a short injection time. Injecting from a desalted solution can further help to sharpen the injected band by sample stacking (**17**). In microfabricated channels, where the starting zone dimensions are given by the shape of the injection loop, a narrow injection plug can be achieved by a proper microdevice design (**18**).

The effect of injection length and size of the detection window on the minimum migration path X needed for the total separation of two zones is schematically shown in **Fig. 1**. Here, the separation of a faster moving component 2 from a slower moving species 1 is depicted in the distance-time scheme. If all other sources of dispersion are neglected, the total width of a separating zone is given by the length of a sample plug injected into the separation capillary. It would seem that both components injected as a zone of a length L_{S1} , are completely separated at a separation distance A . However, the distance-time record of a detector response (shaded areas) at this region shows that the zones are not resolved completely in time dimension. It is evident that the length of a detection window, L_D , contributes to the total width of the zone detected at a given position in time. Therefore, a longer separation path X_B is needed for the total time-separation of both zones. This situation is depicted in region B. Here, the rear boundary of the faster migrating zone 2 is leaving, and the front boundary of slower migrating zone 1 is entering the detection window at the same time. If the lengths of a detection window and an injection plug are reduced to lower values of L_{D2} and L_{S2} (region C), the minimum separation path X_C and the migration time t_C are reduced as well. The

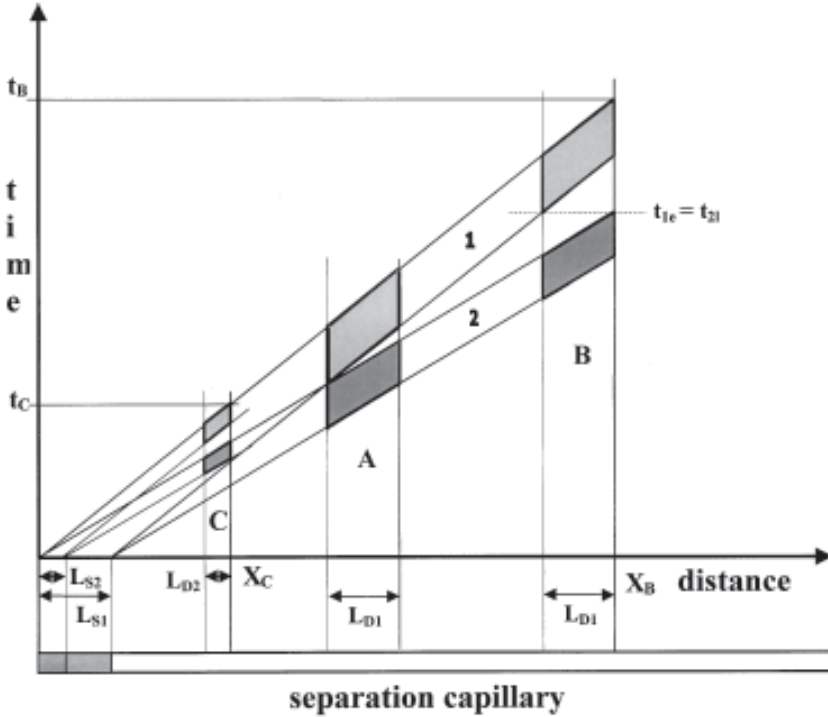


Fig. 1. Effect of lengths of injection zone and detection window on the minimum migration path, space-time scheme of the separation. l_i , l_d injection zone and detection window length, respectively.

minimum separation distance can be evaluated using the above mentioned equality between the times t_{2l} and t_{1e} , at which zones 2 and 1 are leaving and entering the detection window, respectively.

$$t_{2l} = t_{1e} \quad (4)$$

Both times can be expressed as ratios of the migration paths and the respective velocities. The distances between the injection point of the capillary and the rear boundaries of the zones are taken as the migration paths. Then, with respect to **Eq. 1**, we can write:

$$\frac{X}{E\mu_2} = \frac{X - (L_D + L_S)}{E\mu_1} \quad (5)$$

This relationship can be rearranged to:

$$X = (L_D + L_S)/\alpha \quad (6)$$

Hence, the minimum migration path needed for complete separation of two compounds with similar mobility values is proportional to the sum of the lengths of injec-

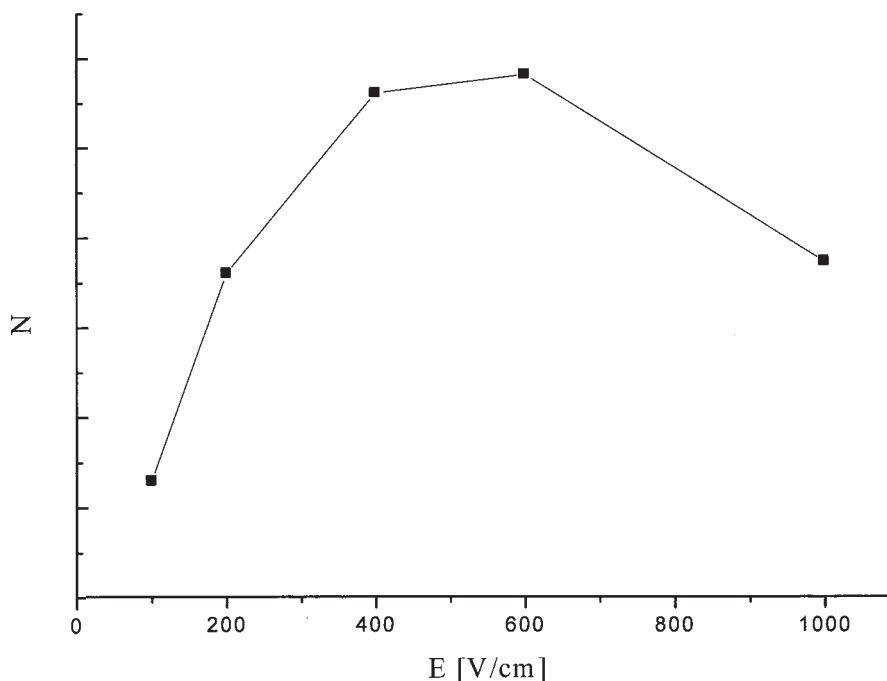


Fig. 2. The dependence of the separation efficiency N on the applied electric field strength E for the 603-bp fragment of the Φ X174/*Hae*III digest. Experimental conditions: 50 μ m id \times 3-cm capillary (DB-1, J&W Scientific, CA), 1% methyl cellulose in a background electrolyte of 40 mM Tris-HCl, 40 mM TAPS, pH 8.4. Capillary temperature is 22°C.

tion plug and the detection window, and is inversely proportional to the separation selectivity.

1.3. Diffusion Dispersion

Since the contribution of diffusion is directly proportional to the time of analysis, faster separation will result in a lower longitudinal diffusion and, consequently, in higher separation efficiencies. The faster the separation times, the less important the effects of diffusion are on the separation efficiencies.

1.4. Thermal Dispersion

In analogy to the diffusion dispersion, the thermal dispersion is also a function of the analysis time. But, in contrast to the diffusion dispersion, thermal dispersion scales with the 6th power of the applied electrical field strength, (19). Thus, when increasing the separation speed by higher electric field strength, two opposing forces are at work. As the applied field strength increases, the diffusion band broadening decreases; however, the thermal dispersion increases. When the separation efficiency is plotted against the applied electric field strength an optimum region of the separation field strength can be found. This is shown in Fig. 2. In practice, depending on the size of the DNA

Table 1
System Optimization Parameters

Parameter	Optimization
σ_{det}^2	Focus light to have small detection spot
σ_{inj}^2	Inject narrow sample plug (inject for short time/use sample stacking)
σ_{therm}^2	Use of short effective capillary length (1–10 cm, depending on resolution needed)
σ_{diff}^2	Application of optimum electric field strength (300–800 V/cm)
σ_{other}^2	High frequency data acquisition system, use of coated capillaries

fragments and the conductivity of the separation matrix this optimum will typically be between 300 and 800 V/cm. It should be noted, that in separations with high selectivity (large differences in sizes of the separated DNA fragments), higher field strength can be used to further increase the separation speed.

1.5. Other Sources of Dispersion

Other sources of dispersion relate to adsorption of the analyte onto the capillary wall, to electroosmotic mixing, to nonhomogeneity of the electric field strength due to the sample matrix ions, or to insufficient speed of the acquisition of data. Fortunately, the negatively charged DNA molecules mostly do not adsorb significantly on the column walls, and most of the hydrophilic surface coatings developed for CE (20) will eliminate the adsorption completely. The surface coating and the use of viscous separation media also eliminate electroosmosis. Electromigration dispersion is typically minimized by sample cleanup and by short injection times. Data acquisition with more than 100 data points per second is adequate for recording peak widths down to 0.1 s, with a total analysis time of few seconds. Most of the standard A/D boards will be sufficient for the data collection.

1.6. Dynamic Structure of DNA

For argument, the DNA fragment is assumed to be a static molecule. However, its molecular orientation under the influence of high electric field in entangled polymer solution can change its diffusion coefficient and its electrophoretic mobility. This effect can be significant especially in case of larger DNA fragments (15). In practice, optimum conditions for fast separations can easily be determined experimentally. **Table 1** lists the parameters, which can be optimized to achieve high-speed DNA separations in entangled polymer solutions.

2. Materials

2.1. Capillary Electrophoresis

1. Fast capillary, fused silica (effective length): 3 cm \times 50 μ m (id), (DB-1, J&W Scientific, CA).
2. Capillary 6.3: 12.1 cm \times 50 μ m id.
3. Constant denaturant capillary electrophoresis (CDCE): Capillary, 7 cm \times 50 μ m (id), coated with poly(vinyl alcohol) (PVA).

4. 1% methylcellulose in 40 mM Tris-base, 40 mM TAPS, pH 8.4 background electrolyte.
5. Electrophoresis buffer: 40 mM Tris-base, 40 mM TAPS, pH 8.4, 1 $\mu\text{g/mL}$ ethidium bromide (EtBr).
6. Standard DNA: $\Phi\text{X174}/\text{HaeIII}$ digest.
7. DNA size standard (Boehringer VIII).
8. $(\text{CA})_{-18}$ microsatellite repeat polymorphism in the *FcER1 β* gene.
9. Mitochondrial DNA.
10. Agarose sieving medium: 4% solution of Agarose BRE (FMC Rockland, ME) in 0.1 M Tris-base, 0.1 M TAPS, pH 8.4 and 7 M urea.
11. LPA Separation matrix: 4% linear polyacrylamide (LPA) in 50 mM Tris-base, 50 mM TAPS, pH 8.4.
12. SYBR Green II dye.
13. Fluorescein at a concentration of 10^{-8} M.
14. 1X TBE buffer: 89 mM Tris-base, 89 mM boric acid, 1 mM EDTA, pH 8.8.

2.2. Chip Electrophoresis

1. Electrophoresis chip with integrated electrochemical detection.
2. Sieving medium: 0.75% (w/v) hydroxyethyl cellulose in 1X TBE buffer, pH 8.8 with 1 μM EtBr.
3. DNA: *RsaI*-digested HFE amplicons.
4. Standard DNA: $\Phi\text{X174}/\text{HaeIII}$ digest.
5. *Salmonella* PCR product.

3. Methods

3.1. Examples of Fast DNA Separations

1. This section illustrates the potential of CE for ultra-fast separations. CE decreases the analysis time typically by ten times compared to standard slab-gel electrophoresis. Depending on the application, the miniaturized CE and microfabricated electrophoresis systems can further decrease the analysis time to tens of seconds or less (16).

3.2. Double-Stranded DNA

1. **Figure 3** shows the separation of the DNA size standard $\Phi\text{X 174}/\text{HaeIII}$, which contains 11 DNA fragments ranging from 72 to 1352 bp. In this example, a coated capillary was used to prevent band broadening by DNA-wall interactions. A high frequency data acquisition system allowed a sampling rate of 100 Hz, ensuring a sufficient number of points to define the bands, which are 0.1–0.2 s wide. In order to achieve resolution of the closest migrating fragments (271 bp/281 bp) on a 3-cm long column, a very narrow sample plug is injected with the aid of a fast switching high-voltage power supply (16). A sample plug width of less than 100 μm can be injected into the capillary during a 100-ms electromigration injection. Under these conditions, baseline resolution of the 271-bp/281-bp bands is achieved in less than 30 s. The insert of **Fig. 3** shows the deleterious effect of a longer injection time on the peak resolution.
2. The speed of CE can be applied to the development of DNA diagnostic methods for molecular identification of hereditary diseases or cancer. The ultra-fast CE systems utilizing short electrophoresis columns (length of several centimeters or less) will allow for a variety of high-throughput DNA diagnostics methodologies (21–23).
3. An example of the application of short capillaries in clinical diagnostics is shown in **Fig. 4**. *FcER1 β* is a high affinity glycoprotein receptor for IgE located on chromosome 11

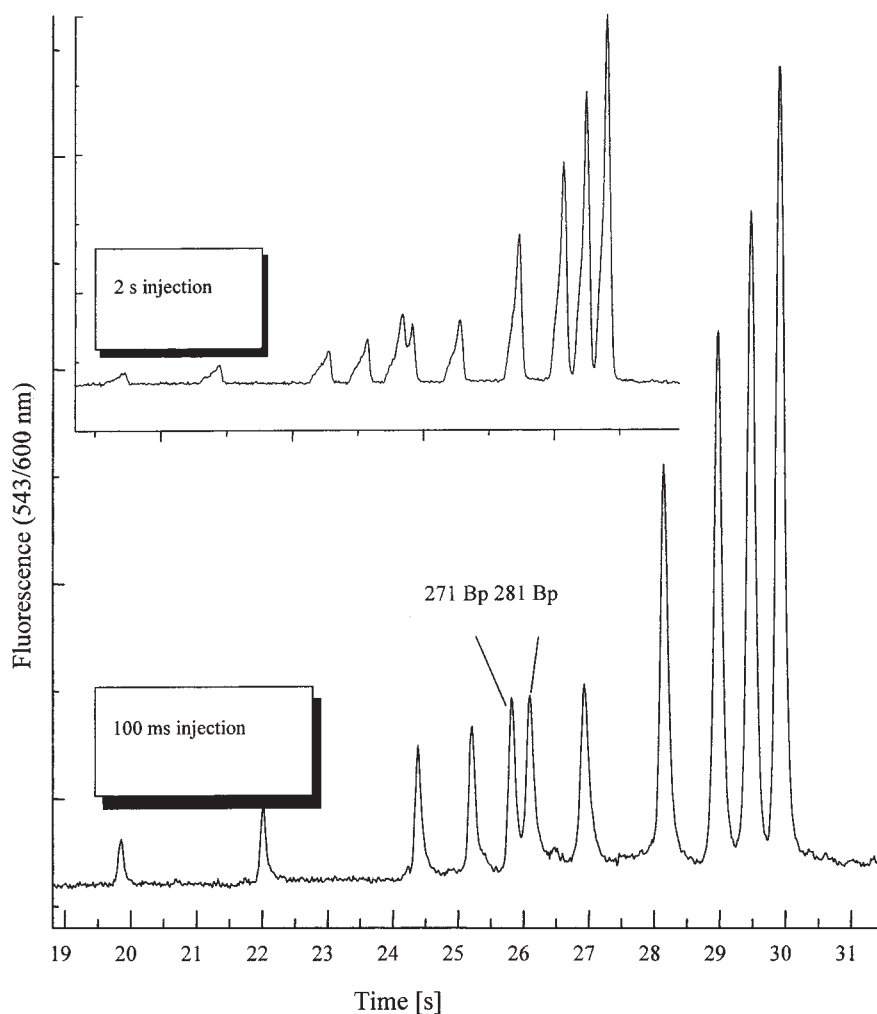


Fig. 3. Separation of Φ X174/*Hae*III digest with 3-s and a 100-ms electrokinetic injection. Experimental conditions: 50- μ m id capillary (DB-1, J&W Scientific, CA). Separation distance: 3 cm. Separation matrix: 1% methyl cellulose in 40 mM Tris-base, 40 mM TAPS, pH 8.4, 1 μ g/mL EtBr. Field strength 800 V/cm. LIF detection (excitation 543 nm/emission 600 nm).

(11q13), and variability of *FcER1 β* gene causes differences in excess of IgE responses, which is a typical feature of atopies such as allergic rhinitis, bronchial asthma, dermatitis, and food allergies. One of the genetic variants identified in the *FcER1 β* locus is a (CA)₁₈ microsatellite repeat polymorphism in intron 5 of the gene. The analysis of the short tandem repeat polymorphism in the *FcER1 β* gene of an heterozygous individual is presented here, covering the (CA)₁₈ repeat which ranges from 112 to 132 bp. The analysis is performed at an electric field strength of 256 V/cm, in a capillary with an effective length of

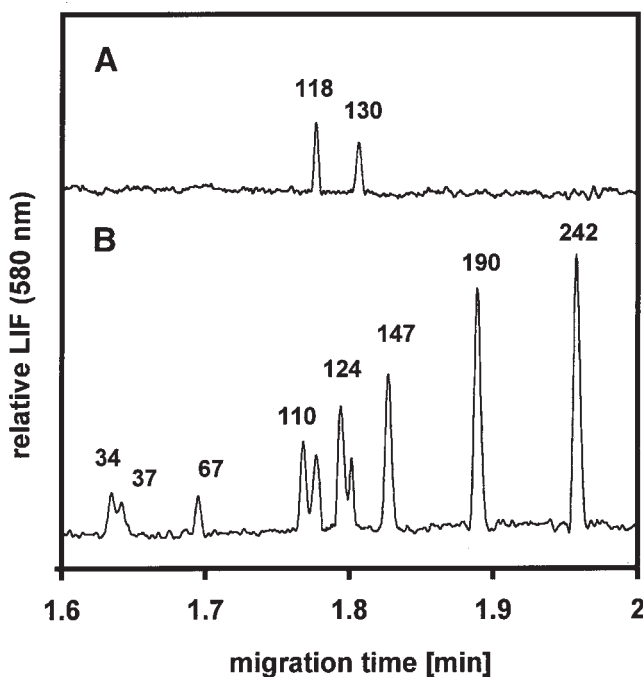


Fig. 4. Detection of $(CA)_{18}$ microsatellite repeat polymorphism in *FcER1 β* gene of a heterozygous individual. LIF detection at 580 nm with fluorescein as an intercalator at a concentration of 10^{-8} M. The separation conditions are 2% Agarose BRE (FMC) in 0.1 M Tris-base, 0.1 M TAPS, pH 8.4. The electrophoresis is at room temperature; injection time is 3 s at 289 V/cm; electrophoresis is at 256 V/cm; capillary 6.3 (12.1) cm, 50 μ m id. The sizes of PCR specific products of the sample (A) were evaluated using an addition of DNA size standard (Boehringer VIII) (B).

6.3 cm in less than 2 min. The respective polymerase chain reaction (PCR) products of sizes 118–130 bp (record A) are identified using an addition of DNA size standard (Boehringer marker VIII) (record B).

3.3. Partially Melted DNA

1. Although there is a difference in the migration behavior of dsDNA, partially melted DNA and ssDNA, most of the system optimization procedures apply to all three types of separations. One application, which takes advantage of differential melting of DNA and is used for the detection of point mutations, is CDCE (24). DNA fragments which contain a mutation usually melt more readily under the influence of a denaturant (heat or urea). Partially melted fragments exhibit a different structure, and therefore, a different migration behavior through an entangled polymer solution.
2. **Figure 5** illustrates the method of screening for an appropriate temperature for the CDCE analysis of a point mutation in a mitochondrial DNA fragment. The sample contains wild-type DNA, mutant DNA, and the two heteroduplex combinations created by boiling-

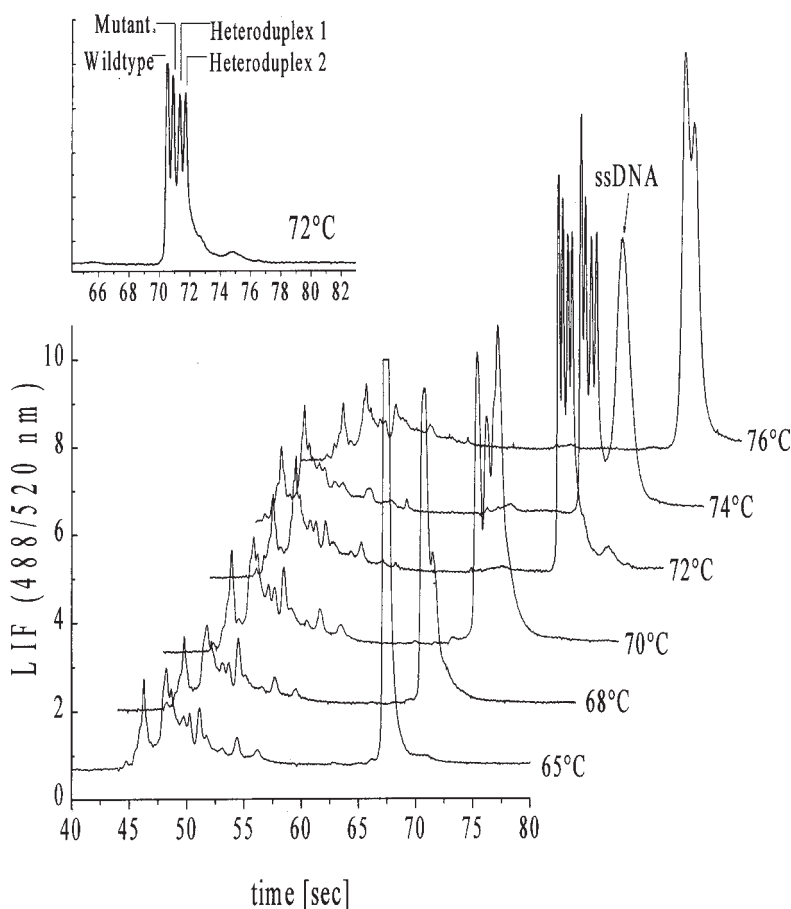


Fig. 5. CDCE of mitochondrial DNA. Capillary 50 μm id \times 7 cm coated with PVA. Separation matrix: 4% LPA in 50 mM Tris-TAPS, pH 8.4. Field strength 600 V/cm ($I = 12 \mu\text{A}$). LIF detection (excitation 488 nm/emission 520 nm).

reannealing steps between the two molecules. The CDCE analysis can be performed in less than 80 s using a 7-cm long capillary and high electric field strength ($E = 600 \text{ V/cm}$). In this example, the temperature screening tests yielded a temperature at which all four different species were separated. The short analysis times helps to rapidly find the optimum temperature for CDCE analysis.

3.4. Single-Stranded DNA

1. DNA sequencing is one area of DNA electrophoresis where the shortening of the analysis time is of key importance. The capillary length cannot be shortened as much as in the previous examples, as extremely high-fragment resolution is required. **Figure 6** shows that up to 300 bases can be separated at 600 V/cm in less than 190 s in a 7-cm long capillary, under optimized separation conditions.

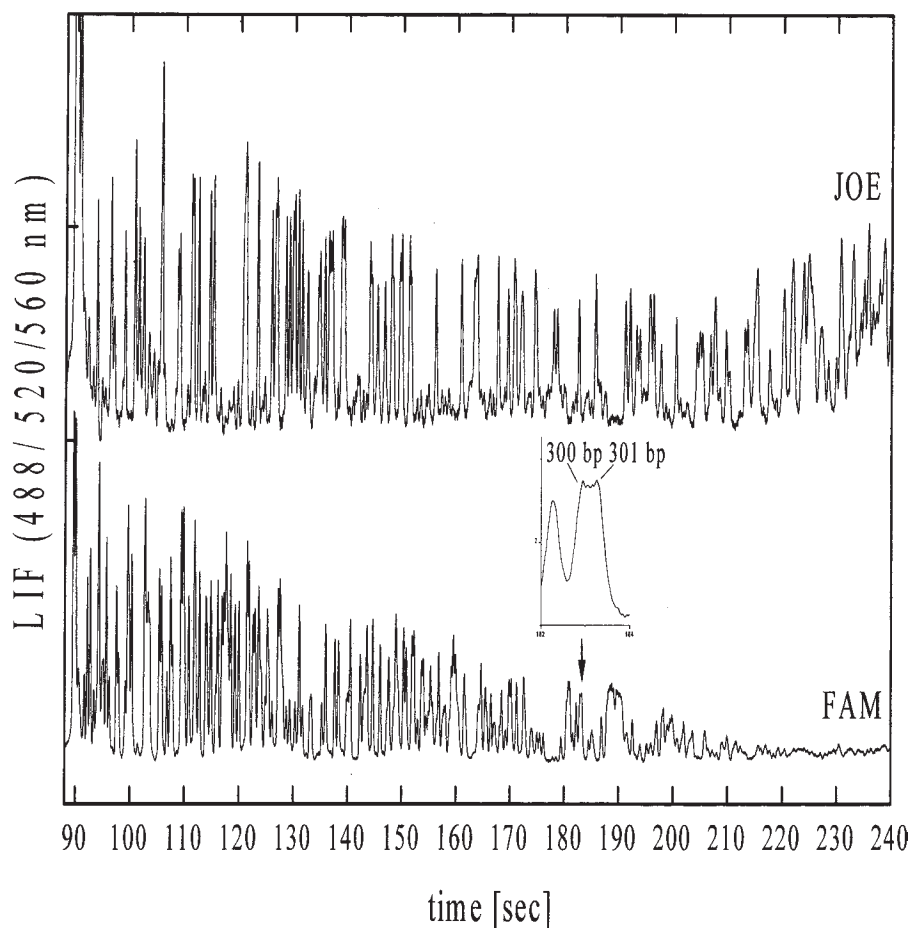


Fig. 6. Fast separation of a sequencing reaction mixture (M13mp18 template). Capillary 50 μm id (PVA coating) \times 7 cm. Separation matrix: 3% LPA, 50 mM Tris-TAPS, pH 8.4. Field strength 600 V/cm, ($I = 7 \mu\text{A}$). LIF detection at (excitation 488 nm/emission 520 nm and 560 nm).

- Polymorphism in the short tandem repeats, consisting from three adjacent repeat regions of CT, CA, and GC and situated between 979 and 1039 position of *Endothelin 1* gene, seems to play a role in transcription regulation. Even though polymorphism does not exactly change the amino acid sequence of the encoded protein, it may have effects on the dynamics of gene expression. Endothelin is a potent vasoconstrictor and, therefore, its gene variability probably impacts the origin of hypertension. The effect of an increased selectivity on the minimum migration path is demonstrated in **Figs. 7 and 8**. These show fast separations under denaturing conditions of DNA fragments amplified from *Endothelin 1* gene of heterozygous individuals.
- The higher separation selectivity of ssDNA fragments enables the use of a capillary with an effective length of 2.5 cm (total length 5 cm), without a loss of resolution. As a result,

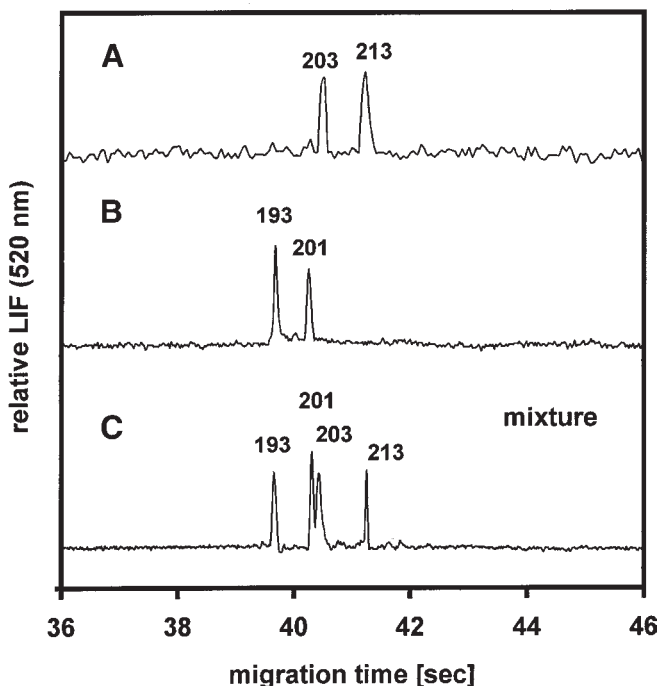


Fig. 7. Detection of CT, CA, GC dinucleotide short tandem repeats polymorphism in *Endothelin 1* gene. Panels (A) and (B): separation of fragments amplified from genomes of heterozygous individuals. Panel (C): mixture of samples A and B. Electrophoresis at 600 V/cm and 60°C in a capillary of 2.5 (5) cm long, 50 μ m id, PVA coated. Sieving medium: 4% sol of Agarose BRE (FMC Rockland, ME) in 0.1 M Tris-base, 0.1 M TAPS, pH 8.4, 7 M urea. Sample is denatured in 0.01 M NaOH at room temperature and stained with SYBR Green II. Injection is for 5 s at 600 V/cm. LIF detection: excitation with argon-ion laser at 488 nm, collected emission is 520 nm.

the resolution needed for the analysis of the dinucleotide repeat polymorphism, can be completed in 42 s. The fragments of lengths of 203 and 213 (panel A) and 193 and 201 nt (panel B) are mixed (panel C) to confirm the resolution between fragments differing by two nucleotides occurs. Heterozygous alleles with the repeats that differ by a single dinucleotide unit were not available (Fig. 7).

4. To increase the speed and resolution yet further, the capillary is held at a temperature of 60°C. This lowers the viscosity of the separation medium and increases its denaturing ability, whereas the thermal energy protects DNA molecules to be stretched under the effect of electric field. Thus, electric field strengths of up to 600 V/cm can be applied. The elevated temperature is conveniently controlled by a 1-cm long heater made of electrically conductive rubber, which also serves as the capillary holder.
5. It is very difficult to achieve denaturation of the DNA fragment carrying the short tandem repeat region of the *Endothelin 1* gene, as the gene has 55% GC pairs. The complementary fragments easily recombine to form heteroduplexes.

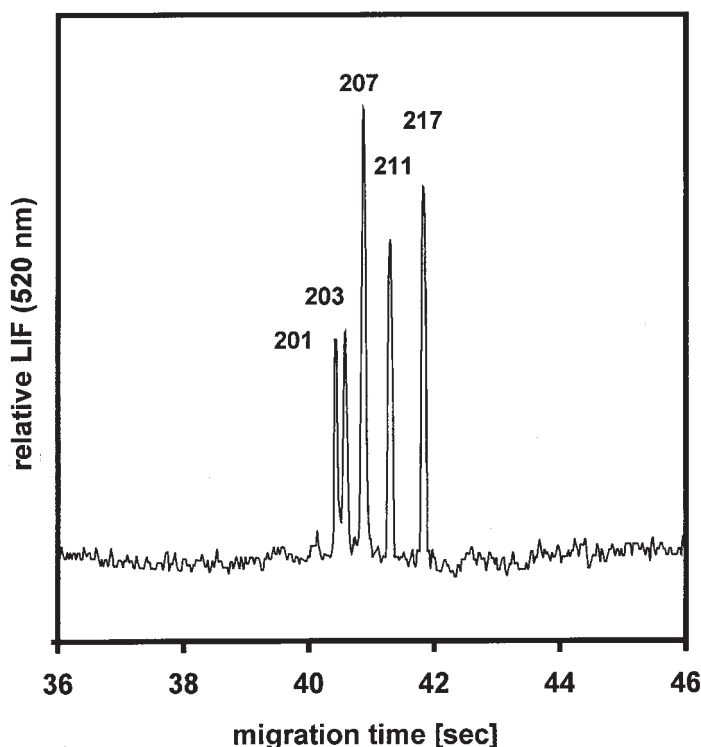


Fig. 8. Fast sizing of a homozygous fragment (203 nt) by using two heterozygous fragments of sizes 207, 217 and 201, 211 nt, respectively. All other conditions are as described in Fig. 7.

6. Dimethylsulfoxide or dimethylformamide, which are generally used for DNA denaturation, are not sufficient for the disruption of short tandem repeats in GC rich regions, and a stronger denaturing agent such as NaOH is used. A solution of 0.01 M NaOH proved to denature the fragments satisfactorily at room temperature. Another advantage of the presence of NaOH in the sample solution is the possibility to use the electrophoretic stacking technique for the injection of a very sharp zone onto the capillary. Based on the isotachophoretic principle, the slower migrating DNA fragments are stacked behind the zone of highly mobile and conductive OH^- anions, and form a much narrower zone than it would for corresponding to the injection times without the ions (25). Thus, as shown in Figs. 7 and 8, even with an injection time of 5 s at the same electric field strength as during the electrophoretic run, the separation window of all fragments is only 2 s.
7. The DNA size-standards are not suitable for calibration, since the migration of fragments amplified from *Endothelin 1* gene is strongly affected by their sequence. Even using strong denaturing conditions, GC rich ssDNA fragments migrate anomalously. Therefore, it is necessary to use known sequence fragments amplified from the *Endothelin 1* genes as size markers for the calibration of unknown samples. In Fig. 8, the size of a homozygous fragment is determined to be 203 nt, by using two heterozygous samples with fragments of sizes 207, 217, and 201, 211 nt, respectively.

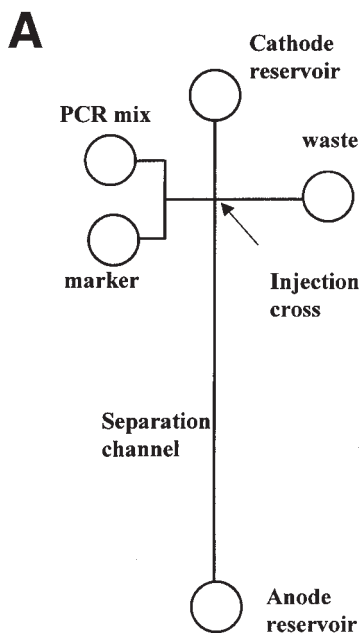


Fig. 9. (A) Schematic of a microchip used for sizing of PCR products with a DNA marker. (B) (a) Electropherogram of the sizing ladder; (b) Electropherogram of PCR products; (c) Electropherogram of the PCR product mixed equally with the sizing ladder. The microchip was filled with 3% (v/v) linear PDMA, the separation length was 2.5 cm. Field strength: 127 V/cm. The numbers denote fragment sizes in base pairs. Adapted with permission from **ref. 28**. Copyright (1998) American Chemical Society (*continued on opposite page*).

8. The use of denaturing electrophoresis in short capillaries with LIF detection resulted in 20-fold reduction in analysis time, when compared to commercially available CE systems.

3.5. DNA Separations on Microfabricated Devices

1. All previous examples utilize a short piece of a fused silica capillary as the separation column. Microfabrication technologies common in electronics are becoming increasingly important for a new generation of analytical instrumentation. Although the first microfabricated instrument (gas chromatograph) was developed some two decades ago (26), it is the current advancement in protein and DNA research that command the development of adequate analytical instrumentation capable of high-throughput analysis of minute amounts of complex samples. Attempts to integrate several of the sample preparation/analysis steps led to the establishment of a new analytical field, that of the micro Total Analytical Systems – “ μ TAS” (27). Mass production of such integrated systems may lead to disposable devices made of inexpensive plastic materials, simplifying routine operation and eliminating sample carry-over or sample cross contamination. In addition, multiple channels on a chip open up the possibility for high-throughput analysis on a microscale. Although the term microdevice (chip, microchip) implies miniaturized size of the separation channel, it should be stressed that since the separation principle remains

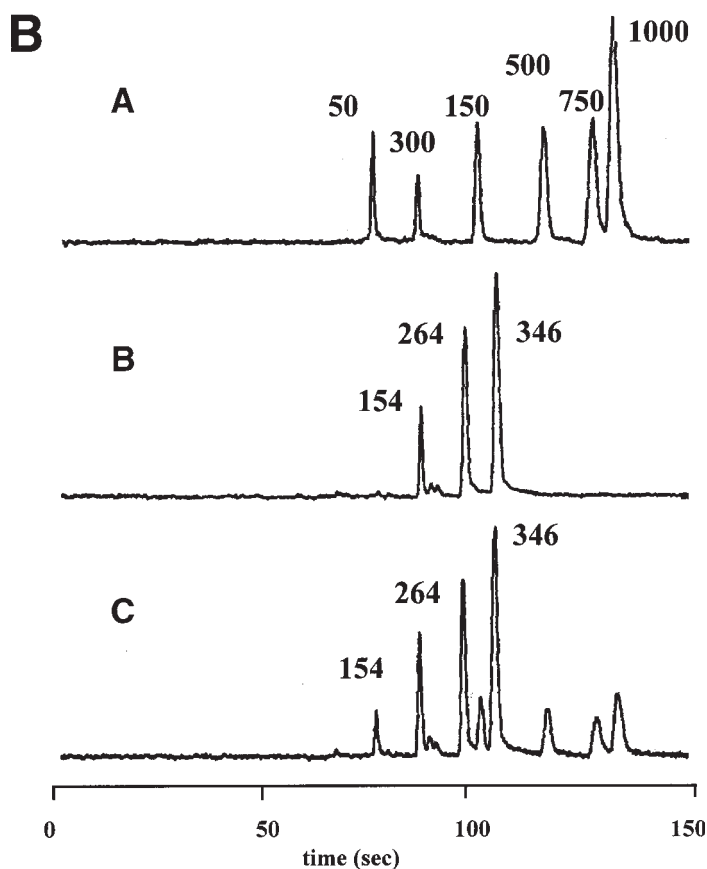


Fig. 9. (continued) (B).

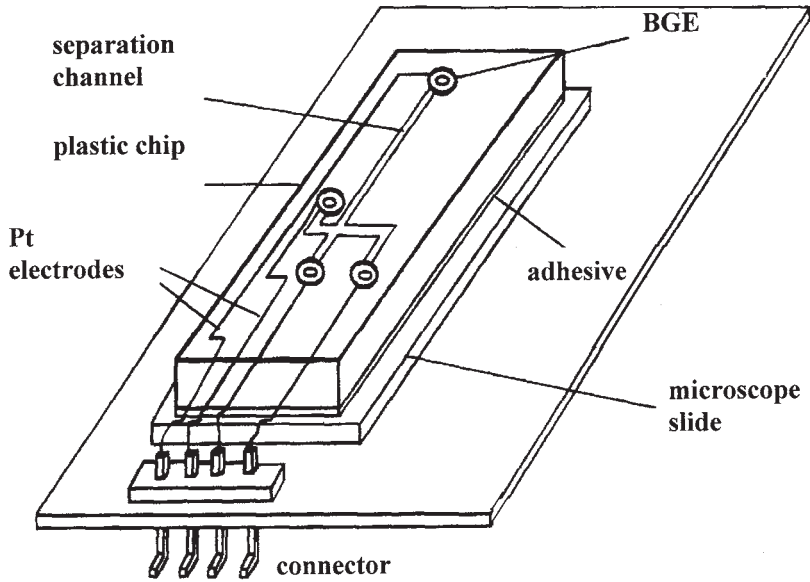
the same, the speed of analysis will be the same, regardless of the type of the separation channel used (capillary or chip).

2. The main advantage of the chip technology is the ease of fabrication of a large number of channels. In comparison to standard instrumentation where all the connections between the different fluid paths are typically made with fluid fittings, zero dead volume channel junctions can easily be microfabricated. For example, precisely defined amounts of the sample can easily be introduced using a simple double T structure microfabricated as an integral part of the separation channel. The resulting significant size reduction will lower analysis cost by increased analysis speed and reduce the consumption of both the sample and separation media. Moreover in principle, sample preparation procedures can also be integrated on the same chip. This is illustrated in **Fig. 9**. **Figure 9A** shows a monolithic microchip device where the steps of cell lysis, multiplex PCR amplification, and electrophoretic analysis are executed sequentially (28). **Figure 9B** shows the separation of a 500-bp region of bacteriophage lambda DNA and 154-, 264-, 346-, 410-, and 550-bp regions of *E. coli* genomic and plasmid DNAs, amplified using a standard PCR protocol.

The electrophoretic analysis of the products is executed in <3 min following completion of the amplification steps, and the product sizing is demonstrated by proportioning the amplified product with a DNA sizing ladder.

3. Since the microfabrication in glass may not be the most cost effective approach for mass production, there is much interest in alternative materials and fabrication procedures. One promising direction is injection-molding using inexpensive plastic materials (29). The strategy for producing the devices involves solution-phase etching of a master template onto a silicon wafer. Then for the consecutive step, a nickel injection mold insert is made from the silicon master by electroforming in nickel. High-resolution separations of dsDNA fragments with total run times of less than 3 min are demonstrated with good run-to-run and chip-to-chip reproducibility. It is expected that injection molded devices could lead to the production of low-cost, single-use electrophoretic chips, suitable for a variety of separation applications including DNA sizing, DNA sequencing, random primary library screening, and/or rapid immunoassay testing. **Figure 10A** shows the complete separation chip with electrodes, electrical connectors, and buffer reservoirs. **Figure 10B** shows the separation of the fragments of a *Hae*III digest of Φ X174 DNA in less than 2.5 min in such a sealed plastic chip.
4. Although the development of microfabricated CE systems is mainly focused on the separation “chip” itself, it is clear that substantial changes to the external parts of the instrumentation will be also necessary, especially changes to the detector. Current advances in solid-state lasers will bring substantial miniaturization of LIF detection. The recently described electrochemical detector, which can be microfabricated as an integral part of the chip itself, is also a promising development (30).
5. Photolithographic placement of the working electrode just outside the exit of the electrophoresis channel provides high-sensitivity electrochemical detection with minimal interference from the separation electric field. Indirect electrochemical detection is used for high-sensitivity DNA restriction fragment and PCR product sizing. These microdevices match the size of the detector to that of the microfabricated separation and reaction devices, bringing to reality the “lab-on-a-chip” concept. **Figure 11** shows the electrophoresis chip with integrated electrochemical detection and corresponding separation of *Salmonella* PCR product (shaded) with 500 pg/mL Φ X174/*Hae*III restriction digest obtained on this chip.
6. As previously mentioned, one of the advantages of the microfabrication is the possibility to make a large number of channels of a variety of shapes with zero dead volume connections. Typical application of this potential may be a CAE microplate that can analyze 96 samples in less than 8 min (31). This CAE chip has been produced by the bonding of 10-cm diameter micromachined glass wafers to form a glass sandwich structure. The microplate with 96 sample wells and 48 separation channels permitted the serial analysis of two different samples on each capillary. Individual samples are addressed with an electrode array positioned above the microplate.
7. The detection of all lanes with high temporal resolution is achieved by using a laser-excited confocal fluorescence scanner. **Figure 12** shows the microdevice used for electrophoretic separation with fluorescence detection for the diagnosis of hereditary hemochromatosis. Electropherograms represent two sequential separations of *Rsa*I-digested *HFE* amplicons. The three genotypes are characterized by a single peak at 140 bp corresponding to the 845G type, a single peak at 111 bp corresponding to the 845A type, and the heterozygote type that exhibits both the 140- and 111-bp peaks.
8. Electrophoretic separation in a short narrow capillary allows extremely fast separations with resolution comparable to, or better than standard slab gel or CE. On the top of the

A



B

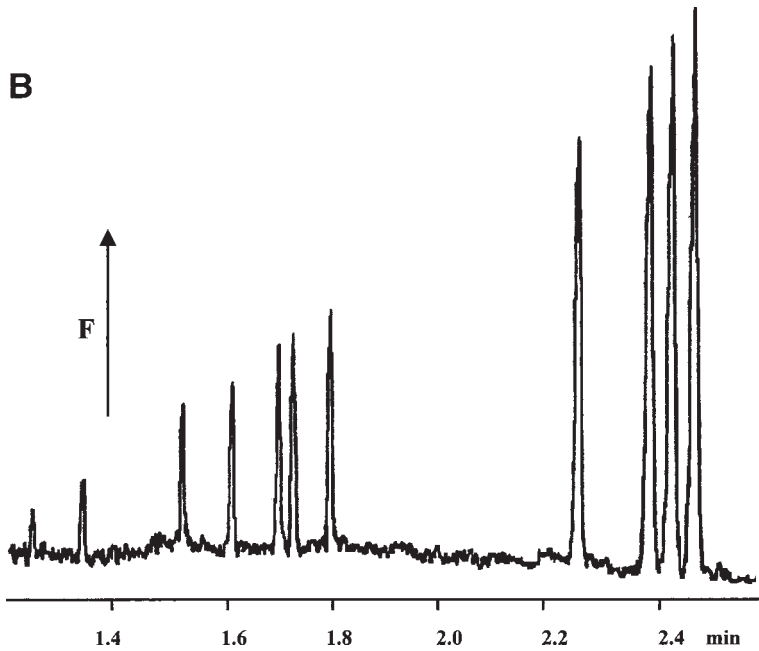


Fig. 10. (A) Completed separation chip with electrodes, electric connectors and buffer reservoirs. (B) Separation of a *Hae*III digest of Φ X174 RF DNA fragments in a sealed plastic chip. Adapted with permission from ref. 29. Copyright (1997) American Chemical Society.

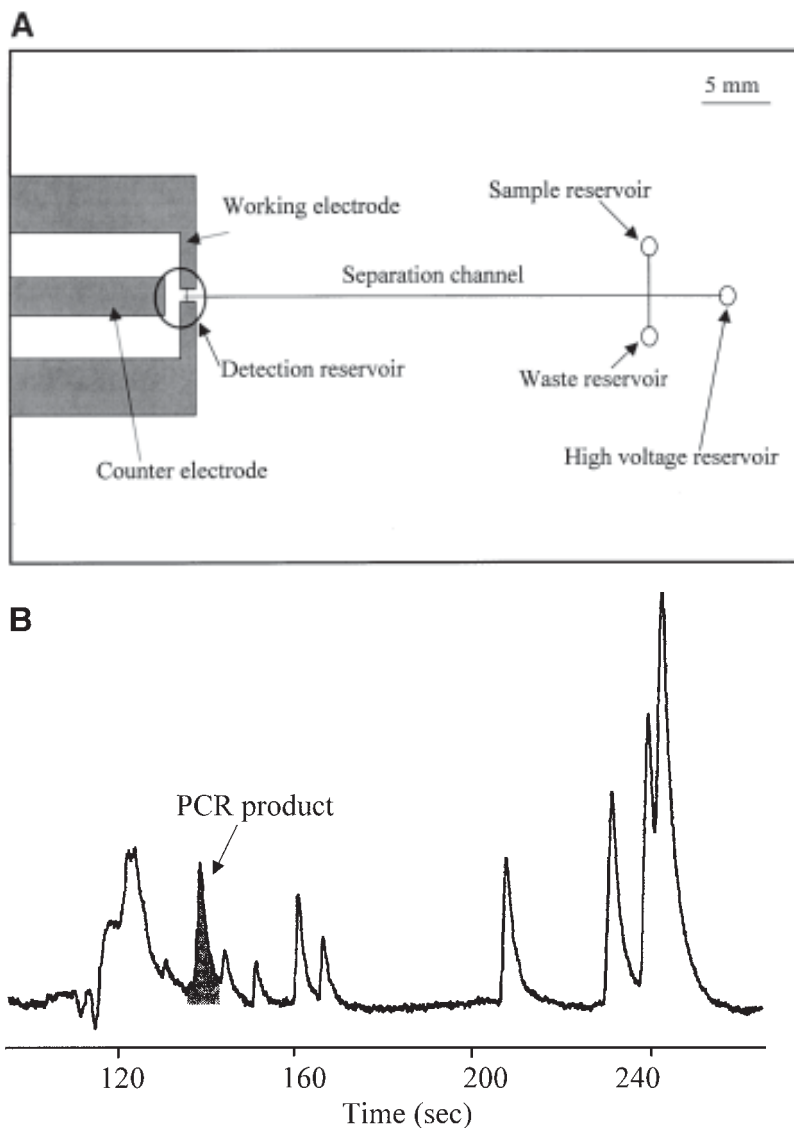


Fig. 11. **(A)** Diagram of an electrophoresis chip with integrated electrochemical detection. **(B)** Separation obtained on this chip of a *Salmonella* PCR product (shaded) along with 500 pg/mL of Φ X174/*Hae*III restriction digest. Adapted with permission from ref. 30. Copyright (1998) American Chemical Society.

analysis speed, the current technology also provides sensitive LIF detection for all critical applications. The maturity of the CE has currently been confirmed by its application for the accelerated completion of the Human Genome Project. It can be also anticipated

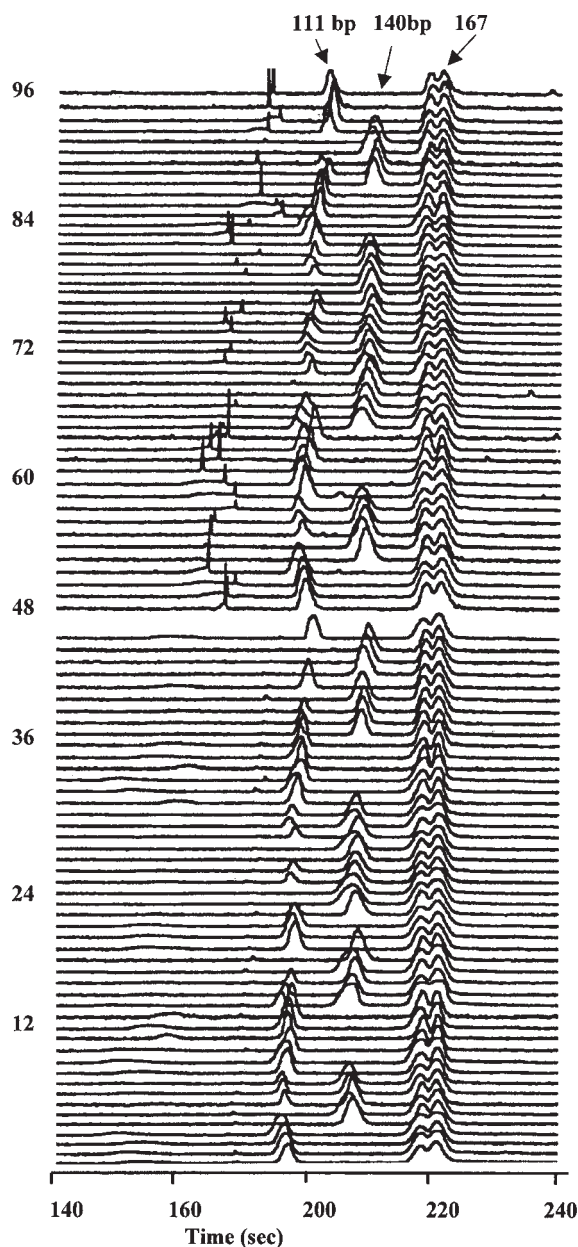


Fig. 12. ACE separations of two sequential "48-samples" of *RsaI*-digested *HFE* amplicons. The three genotypes correspond to a single peak at 140 bp (845G type), 111 bp (845A type) and two peaks at 140 bp and 111 bp (heterozygote). Samples were separated in 10-cm long channels using 0.75% (w/v) hydroxyethyl cellulose in 1X TBE buffer with 1 μ M EtBr. Field strength 300 V/cm. Adapted with permission from **ref. 31**. Copyright (1998) American Chemical Society.

that future development of these microfabricated devices will enable extremely rapid analytical and diagnostic tools, integrating the fast electrophoretic separation methods with microscale sample processing.

Acknowledgments

The preparation of this chapter has been supported by Grants No. 203/00/0772 and 301/97/1192 of the Grant Agency of the Czech Republic, and with support from the Barnett Institute for Contribution #768.

References

1. Shapiro, A. L., Vinuela, E., and Maizel, J. V. (1967) Molecular weight estimation of polypeptide chains by electrophoresis in SDS-polyacrylamide gels. *Biochem. Biophys. Res. Commun.* **28**, 815.
2. O'Farrell, P. H. (1975) High resolution two-dimensional electrophoresis of proteins. *J. Biol. Chem.* **250**, 4007–4021.
3. Sanger, F., Nicklen, S., and Coulson, A. R. (1977) DNA sequencing with chain-terminating inhibitors. *Proc. Natl. Acad. Sci. USA* **74**, 5463–5467.
4. Maxam, A. M. and Gilbert, W. (1977) A new method for sequencing DNA. *Proc. Natl. Acad. Sci. USA* **74**, 560–654.
5. Andrews, A. T. (1986) *Electrophoresis: Theory, Technique, and Biochemical and Clinical Applications*, 2nd ed., Clarendon Press, Oxford.
6. Rickwood, D. and Hames, B. D. (eds.), (1990) *Gel Electrophoresis of Nucleic Acids*, 2nd ed., Oxford University Press, Oxford, New York.
7. Deyl, Z. (ed.), (1979) Electrophoresis: Part A: techniques. *J. Chromatogr. Library* **18**, Elsevier, Amsterdam.
8. Hjertén, S. (1967) Free zone electrophoresis. *Chromatogr. Rev.* **9**, 122–219.
9. Virtanen, R. (1974) Zone electrophoresis in a narrow-bore tube employing potentiometric detection. *Acta Polytech. Scand.* **123**, 1–67.
10. Mikkers, F. E. P., Everaerts, F. M., and Verheggen, Th. P. E. M. (1979) High performance zone electrophoresis. *J. Chromatogr.* **169**, 11–20.
11. Jorgenson, J. W. and Lukacs, K. D. (1981) Zone electrophoresis in open tubular glass capillaries. *Anal. Chem.* **53**, 1298–1303.
12. Karger, B. L., Chu, Y., and Foret, F. (1995) Capillary electrophoresis of proteins and nucleic acids. *Annu. Rev. Biophys. Biomol. Struct.* **24**, 579–610.
13. Grossbach, U. (1965) Acrylamide gel electrophoresis in capillary columns. *Biochim. Biophys. Acta* **107**, 180–182.
14. Hyden, H., Bjurström, K., and McEwen, B. (1966) Protein separation at the cellular level by micro disc electrophoresis. *Anal. Biochem.* **17**, 1–15.
15. Slater, G. W., Mayer, P., and Grossman, P. D. (1995) Diffusion, Joule heating, and band broadening in capillary gel electrophoresis of DNA. *Electrophoresis* **16**, 75–83.
16. Mueller, O., Minarik, M., and Foret, F. (1998) Ultrafast DNA analysis by capillary electrophoresis/laser-induced fluorescence detection. *Electrophoresis* **19**, 1436–1444.
17. Chan, K. C., Muschik, G. M., and Issaq, H. J. (1997) High-speed electrophoretic separation of DNA fragments using a short capillary. *J. Chromatogr.* **695**, 113–115.
18. Woolley, A. T., Sensabaugh, G. F., and Mathies, R. A. (1997) High-speed DNA genotyping using microfabricated capillary array electrophoresis chips. *Anal. Chem.* **69**, 2181–2186.

19. Foret, F., Deml, M., and Bocek, P. (1988) Capillary zone electrophoresis: quantitative study of the effects of some dispersive processes on the separation efficiency. *J. Chromatogr.* **452**, 601–613.
20. Hjertén, S. (1985) High-performance electrophoresis: elimination of electroendosmosis and solute adsorption. *J. Chromatogr.* **347**, 191–198.
21. Liu, S., Shi, Y., Ja, W. W., and Mathies, R. A., (1999) Optimization of high-speed DNA sequencing on microfabricated capillary electrophoresis channels. *Anal. Chem.* **71**, 566–573.
22. Schmalzing, D., Adourian, A., Koutny, L., Ziaugra, L., Matsudaira, P., and Ehrlich, D. (1998) DNA sequencing on microfabricated electrophoretic devices. *Anal. Chem.* **70**, 2303–2310.
23. Kleparnik, K., Mala, Z., Havac, Z., Blazkova, M., Holla, L., and Bocek, P. (1998) Fast detection of a (CA)₁₈ microsatellite repeat in IgE receptor gene by capillary electrophoresis with laser induced fluorescence detection. *Electrophoresis* **19**, 249–255.
24. Khrapko, K., Hanekamp, J., Thilly, W., Belenky, A., Foret, F., and Karger, B. L. (1994) Constant denaturant capillary electrophoresis (CDCE) - a high resolution approach to mutational analysis. *Nucleic Acids Res.* **22**, 364–369.
25. Bocek, P., Deml, M., Gebauer, P., and Dolnik, V. (1988) *Analytical Isotachophoresis*. VCH Verlagsgesellschaft, Weinheim.
26. Terry, S. C., Jerman, J. H., and Angell, J. B. (1979) A gas chromatographic analyzer fabricated on a silicon wafer. *IEEE Trans. Electron. Devices* **26**, 1880–1886.
27. Manz, A., Harrison, D. J., Verpoorte, E. M. J., Fetting, J. C., Paulus, A., Ludi, H., et al. (1992) Planar chips technology for miniaturization and integration of separation techniques into monitoring systems. Capillary electrophoresis on a chip. *J. Chromatogr.* **593**, 253–258.
28. Waters, L. C., Jacobson, S. C., Kroutchinina, N., Khandurina, J., Foote, R. S., and Ramsey, J. M. (1998) Microchip device for cell lysis, multiplex PCR amplification, and electrophoretic sizing. *Anal. Chem.* **70**, 158–162.
29. McCormick, R. M., Nelson, R. J., Alonso-Amigo, M. G., Benvegna, J., and Hooper, H. H. (1997) Microchannel electrophoretic separations of DNA in injection-molded plastic substrates. *Anal. Chem.* **69**, 2626–2630.
30. Woolley, A. T., Lao, K. Q., Glazer, A. N., and Mathies, R. A. (1998) Capillary electrophoresis chips with integrated electrochemical detection. *Anal. Chem.* **70**, 684–688.
31. Simpson, P. C., Roach, D., Woolley, A. T., Thorsen, T., Johnston, R., Sensabaugh, G. F., et al. (1998) High-throughput genetic analysis using microfabricated 96-sample capillary array electrophoresis microplates. *Proc. Natl. Acad. Sci. USA* **95**, 2256–2261.



<http://www.springer.com/978-0-89603-765-6>

Capillary Electrophoresis of Nucleic Acids

Mitchelson, K.R.; Cheng, J. (Eds.)

2001, XX, 408 p., Hardcover

ISBN: 978-0-89603-765-6

A product of Humana Press